Food Chemistry: X 22 (2024) 101341

Contents lists available at ScienceDirect

Food Chemistry: X

journal homepage: www.sciencedirect.com/journal/food-chemistry-x

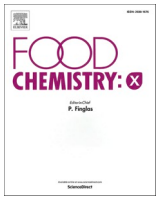

Low-frequency alternating magnetic field and $CaCl_2$ influence the physicochemical, conformational and gel characteristics of low-salt myofibrillar protein

Shengming Zhao [a,c,*], Yu Liu [a,c], Liu Yang [a,c], Yanyan Zhao [a,c], Mingming Zhu [a,c], Hui Wang [a,c], Zhuangli Kang [b], Hanjun Ma [a,c,*]

[a] School of Food Science and Technology, Henan Institute of Science and Technology, PR China
[b] School of Tourism and Cuisine, Yangzhou University, Yangzhou 225127, PR China
[c] Research and Experimental Base for Traditional Specialty Meat Processing Techniques of the Ministry of Agriculture and Rural Affairs of the People's Republic of China, PR China

ARTICLE INFO

Keywords:
Myofibrillar protein
Low-frequency alternating magnetic fields
$CaCl_2$

ABSTRACT

In this study, the improvement mechanism of low-frequency alternating magnetic field (LF-AMF, 5 mT, 3 h) combined with calcium chloride ($CaCl_2$, 0–100 mM) on the gel characteristics of low-salt myofibrillar protein (MP) was investigated. LF-AMF combined with 80 mM $CaCl_2$ treatment increased solubility (32.71%), surface hydrophobicity (40.86 μg), active sulfhydryl content (22.57%), water-holding capacity (7.15%). Besides, the combined treatment decreased turbidity, particle size and intrinsic fluorescence strength of MP. Fourier transform infrared spectroscopy (FT-IR) results indicated that the combined treatment altered the secondary structure of MP by increasing β-sheet and β-turn, and reducing α-helix and random coil. The combined treatment also induced a high G' value and shortened T_2 relaxation time for forming a homogeneous and compact gel structure. These results revealed that LF-AMF combined $CaCl_2$ treatment could as a potential approach for modifying the gel characteristics of low-salt MP.

1. Introduction

The desirable qualities of processed meat products are highly dependent on the functional properties of muscle proteins. Myofibrillary protein (MP) as the primary muscle protein was vital to meat processing (Wang et al., 2020). The solubility of MP is widely considered to be a fundamental attribute of muscle protein for meat production (Wang, Li, Zhang, Luo, & Sun, 2022). Therefore, NaCl (0.47–0.86 M) is commonly used in meat processing to increase the shielding charge and the ionic strength, facilitating the dissolution of MP for forming a desirable gel network structure during the heating process (Li, Zhang, Lu, & Kang, 2021; Wang et al., 2020b). Moreover, NaCl was also used as an indispensable food additive to enhance the flavor and texture properties, and inhibit the growth of pathogenic microorganisms in meat products (Zheng, Han, Ge, Zhao, & Sun, 2019). Nevertheless, increasing evidence suggests that high sodium diets are harmful to human health, particularly in the increasing incidence of hypertension and cardio-cerebrovascular diseases (Zheng et al., 2019). Thus, there is a rising health consumer demand for developing low-sodium meat products. However, a reduction of the NaCl level can reduce the gel strength of MP, leading to the flavor and quality deterioration of meat products (Gao et al., 2022). Thereby, partial replacement of NaCl by non-sodium salt (KCl, $CaCl_2$, $MgCl_2$) and non-thermal processing techniques such as pulsed electric field, ultrasonic and high pressure have been utilized as the major strategies to overcome this challenge (Wang et al., 2022; Wang, Xia, Zhou, Wang, et al., 2020b; Zheng et al., 2019).

Calcium chloride ($CaCl_2$), as a calcium supplement, in addition to improving the nutrition of meat products, can modify the gel characteristics of MP by inducing conformational changes, promoting charge shielding, enhancing protein solubility, and forming salt bridge during thermal gelation (Pan, Guo, Li, Song, & Ren, 2017; Wang, Xia, Zhou, Wang, et al., 2020b; Xiao et al., 2020). $CaCl_2$ has currently been used for NaCl substitution for improving the gel characteristics in low-salt meat products (Wang et al., 2018; Zheng et al., 2019). However, the protein types, calcium concentration, and processing methods might alter the charge balance between proteins affecting the gel characteristics of meat

* Corresponding authors at: School of Food Science and Technology, Henan Institute of Science and Technology, PR China.
E-mail addresses: zhaoshengming2008@126.com (S. Zhao), xxhjma@126.com (H. Ma).

https://doi.org/10.1016/j.fochx.2024.101341
Received 19 January 2024; Received in revised form 25 March 2024; Accepted 29 March 2024
Available online 31 March 2024

proteins (Hu et al., 2022; Pan et al., 2017; Wang et al., 2020a). In addition, excessive use of $CaCl_2$ is associated with decreased functional properties for MP, such as low emulsification, WHC, and vulnerable gel strength (Wang, Xia, Zhou, Wang, et al., 2020b). Hence, reducing use of $CaCl_2$ in low-salt meat products with a specific processing method for without quality deterioration is a growing challenge.

Low-frequency alternating magnetic field (LF-AMF) is a safe and healthy non-thermal treatment method without a medium. The magnetic field is considered an efficient method to induce the formation of 3 D gel network structure of MP and improve gel properties by modifying the MP structure, such as active groups exposure, orientation change of the charged MP molecules, protein unfolding, rearrangement, and cross-linking (Guo et al., 2019; Wang, Zhou, Wang, Li, et al., 2020; Yang et al., 2020). Besides, the combination of water molecule is highly responsible for the natural conformation of proteins. The magnetic field can modify the hydration characteristics of proteins by influencing physicochemical characteristics of water molecules (Yang et al., 2021). However, to our knowledge, no studies concerning the influences of LF-AMF and $CaCl_2$ on gel characteristics of low-salt MP have been explored. In the present study, the impact of LF-AMF (5 mT, 3 h) and $CaCl_2$ (0–100 mM) on the physicochemical, conformational, and gel characteristics of low-salt myofibrillar protein (0.3 M NaCl). Finally, changes in turbidity, particle size, solubility, active sulfhydryl, secondary structure, tertiary structure, WHC, moisture migration, rheological property, and microstructure were evaluated.

2. Materials and methods

2.1. Materials

Pork *longissimus dorsi* (pH, 5.57 ± 0.06; moisture 72.54 ± 1.16%, protein 16.42 ± 0.86%, fat 2.89 ± 0.09%) slaughtered from landrace (approximately 6 months old, 100 ± 5 kg) were purchased from Gaojin group (Xinxiang, China) after 48 h postmortem. Then, the pork *longissimus dorsi* was stored at 4 °C (within 5 h) until extraction of MP. Calcium chloride ($CaCl_2$) was provided by Dean Chemical Co., Ltd. (Tianjin, china). All other chemicals were of analytical grade.

2.2. Extraction of MP

The MP was extracted by the method as reported by Zhao et al. (2022). Briefly, the ground meat (100 g) were homogenized with 4 times volume (*w/v*) of isolation buffer (0.1 M NaCl, 2 mM $MgCl_2$, 1 mM (EGTA), 10 mM KH2PO4/K_2HPO_4, pH 7.0) by a homogenizer (T25, IKA, Germany) at 10000 × g for 1 min. Then, the mixtures were centrifuged (1500 ×*g*, 4 °C) for 0.5 h and the precipitates were harvested. Subsequently, the precipitates were resuspended with 0.1 mol/L NaCl solution at a solid-liquid ratio of 1:4 (g/mL) and then centrifuged (150,000 ×*g*, 4 °C) for 0.5 h (L-80-XP, Beckman, USA). The harvested precipitates were crude MPs and stored at 4 °C until further analysis (within 48 h). PIPES buffer (15 mM, 0.3 M NaCl) containing 0, 20, 40, 60, 80, and 100 mM $CaCl_2$, was used for diluting the MP suspensions, respectively.

2.3. LF-AMF treatment

The MP suspensions (containing 0, 20, 40, 60, 80, and 100 mM $CaCl_2$) were treated by LF-AMF at 5 mT, 4 °C for 3 h in a magnetic field refrigerator (MFI-F1, INDUC Scientific Co., Ltd., Wuxi, China). MP suspensions without LF-AMF treatment were used as a control.

2.4. Preparation of MP gels

After LF-AMF treatment, MP suspensions were diluted to 55 mg/mL by PIPES buffer (15 mM, pH 6.25) were heated (80 °C, 20 min) with a water bath for gelation. Then, the samples were immediately chilled using a cold-water shower and stored at 4 °C overnight before the WHC, gel strength, water distribution, and microstructure were measured.

2.5. Turbidity and particle size

The MP suspensions were diluted to 1 mg/mL by PIPES buffer (15 mM, pH 6.25) and the turbidity was determined by a spectrophotometer (UT-1810, Persee Co. Ltd., Beijing, China) at 660 nm, and the particle size of MP suspensions (0.1 mg/mL) was determined by a nanoparticle size analyzer (Zetasizer Nano-ZS90, Malvern Instruments Ltd., Worcester shire, UK) (Zhao, Li, et al., 2022).

2.6. Solubility

The MP suspensions were diluted to 5 mg/mL by PIPES buffer (15 mM, pH 6.25) and centrifuged at 8000 ×*g* for 20 min (L-80-XP, Beckman, USA) and the solubility was measured using the Coomassie brilliant blue method for evaluating the protein content (Wang, Xia, Zhou, Wang, et al., 2020b). The solubility was defined as follows:

$$Solubility\ (\%) = \frac{\text{Protein content of supernatant}}{5\ \text{mg/mL}} \times 100\%$$

2.7. Surface hydrophobicity

Briefly, 1 mL MP suspensions (2 mg/mL) and 200 μl BPB (1 mg/mL) were mixed well for 10 min. Then, after centrifugation at 6000 ×*g* for 15 min, the absorbance of the supernatant was determined at 595 nm. The BPB bound was defined as follows:

$$BPB\ bound\ (\mu g) = 200 \times \frac{\left(A_{control} - A_{sample}\right)}{A_{control}}$$

2.8. Active sulfhydryl content

1.5 mL MP samples (5 mg/ml) were incorporated with 10 ml Tris-glycine buffer (pH 8), 50 μL Ellman reagent, and mingled for 5 min. Then, the mixture was reacted for 60 min at 25 °C and centrifugated at 10000 × g for 10 min (Yang et al., 2021). The absorbance of the supernatant was determined at 412 nm with a spectrophotometer (UT-1810, Persee Co. Ltd., Beijing, China).

$$Active\ sulfhydryl\ content\ (\mu mol/g) = \frac{73.53 \times A_{412\ nm} \times D_{dilution\ multiple}}{C_{protein\ concentration}}$$

2.9. Fourier transform infrared spectroscopy (FTIR)

The MP samples were monitored by a Fourier infrared spectrometer (TENSOR27, Bruker Optics Co., Ltd., Bremen, Germany). The setting of scanning range, resolution, and scan times was 4000 cm^{-1}-400 cm^{-1}, 4 cm^{-1}, and 32 times, respectively. Omnic 8.0 and Peakfit 4.12 software were used for spectrum analysis (Zhao et al., 2022).

2.10. Intrinsic fluorescence spectroscopy

The intrinsic tryptophan fluorescence spectra of MP suspensions (0.1 mg/ml) were monitored using a Cary Eclipse spectrofluorometer (Cary Eclipse G9800A, Agilent Ltd., Kuala Lumpur, Malaysia) according to Xiao et al. (2020). The setting of excitation wavelength, scan range, and slit width was 295 nm, 300–400 nm, and 5 nm, respectively.

2.11. Gel properties

2.11.1. WHC

The MP samples were cooked at 85 °C for 15 min. Then, 10 g of gel samples (m_1) were centrifugated (6000 × g, 4 °C, 15 min) and weighed as m_2. The WHC was calculated based on the following formula (Ma et al., 2012):

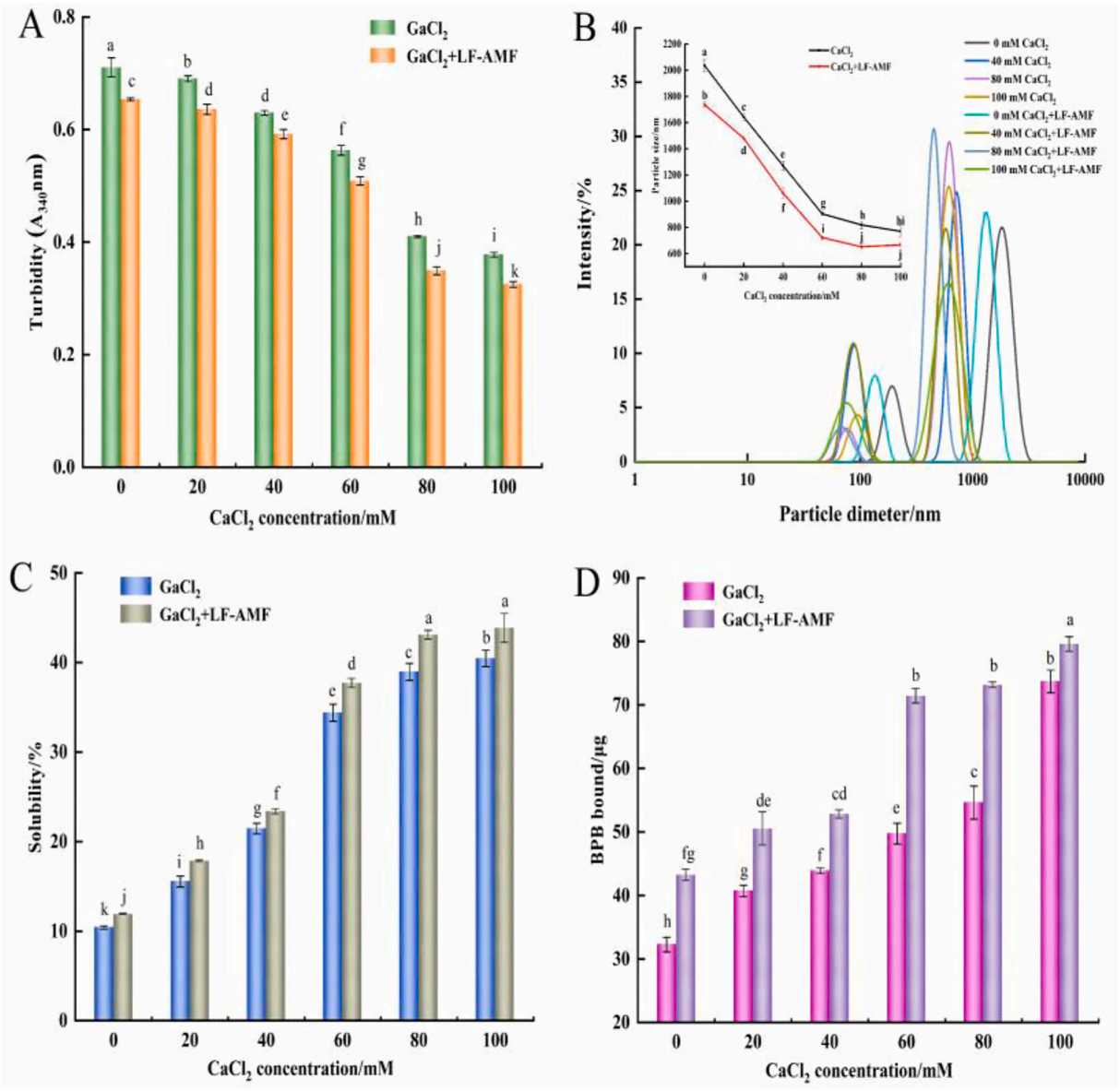

Fig. 1. Effects of LF-AMF combined with $CaCl_2$ on the turbidity (A), particle size (B), solubility (C) and surface hydrophobicity (D) of MP. Different letters (a-k) indicate significant differences among groups ($P < 0.05$).

$$WHC\ (\%) = \frac{m_2}{m_1} \times 100$$

2.11.2. Gel strength

The analysis of gel strength of gel samples was carried out by a texture analyzer (TA-XT plus, Stable Micro Systems, Surrey, UK) using a P/0.5 probe in Return To Start mode. The setting of test parameters was as follows: test speed, 2 mm/s; compression distance, 4 mm; trigger force, 5 g (Wu et al., 2021).

2.11.3. Low-field nuclear magnetic resonance (LF-NMR)

Moisture distribution and migration of MP were monitored as previously documented by Guo, Li, Wang, and Zheng (2019). The samples (1.5 cm × 1.5 cm × 2 cm cubes) were placed into a low-field NMR analyzer (Model PQ001, Niumag Electric Corporation, Shanghai, China). The Carr-Purcell-Meiboom-Gill pulse sequence with a τ value of 350 μs and a proton resonance frequency of 22.6 MHz at 32 °C were used for analyzing spin-spin relaxation times (T_2). The inversion fitting software was used to determine the T_2 relaxation times and corresponding water population.

2.11.4. Dynamic rheology

The dynamic rheology was measured by a dynamic rheometer (HAAKE MARS III, Thermo Fisher Scientific Ltd., Karlsruhe, Germany) equipped with a P35 TiL probe (1 mm plate gap). Dynamic temperature scanning (20–80 °C) parameters were as follows: initial temperature, 20 °C; heating rate, 2 °C/min; oscillation frequency, 1 Hz. Dynamic frequency scanning (0–10 Hz) parameters were as follows: strain, 1%; temperature, 20 °C.

2.11.5. Microstructure

The MP samples were pretreated according to the method reported by Wang, Zhou, Wang, Li, et al. (2020). The MP samples were fixed in a solution of 2.5% glutaraldehyde for 24 h, then dehydrated in different volume gradients (50%, 70%, 90%, 95%, and 100%) of ethanol for 15 min. Subsequently, the samples were vacuum dried and gold-coated to observe the microstructures using a scanning electron microscope (Quanta 200, FEI Co., Ltd., Portland, USA) at a magnification of 2000 × .

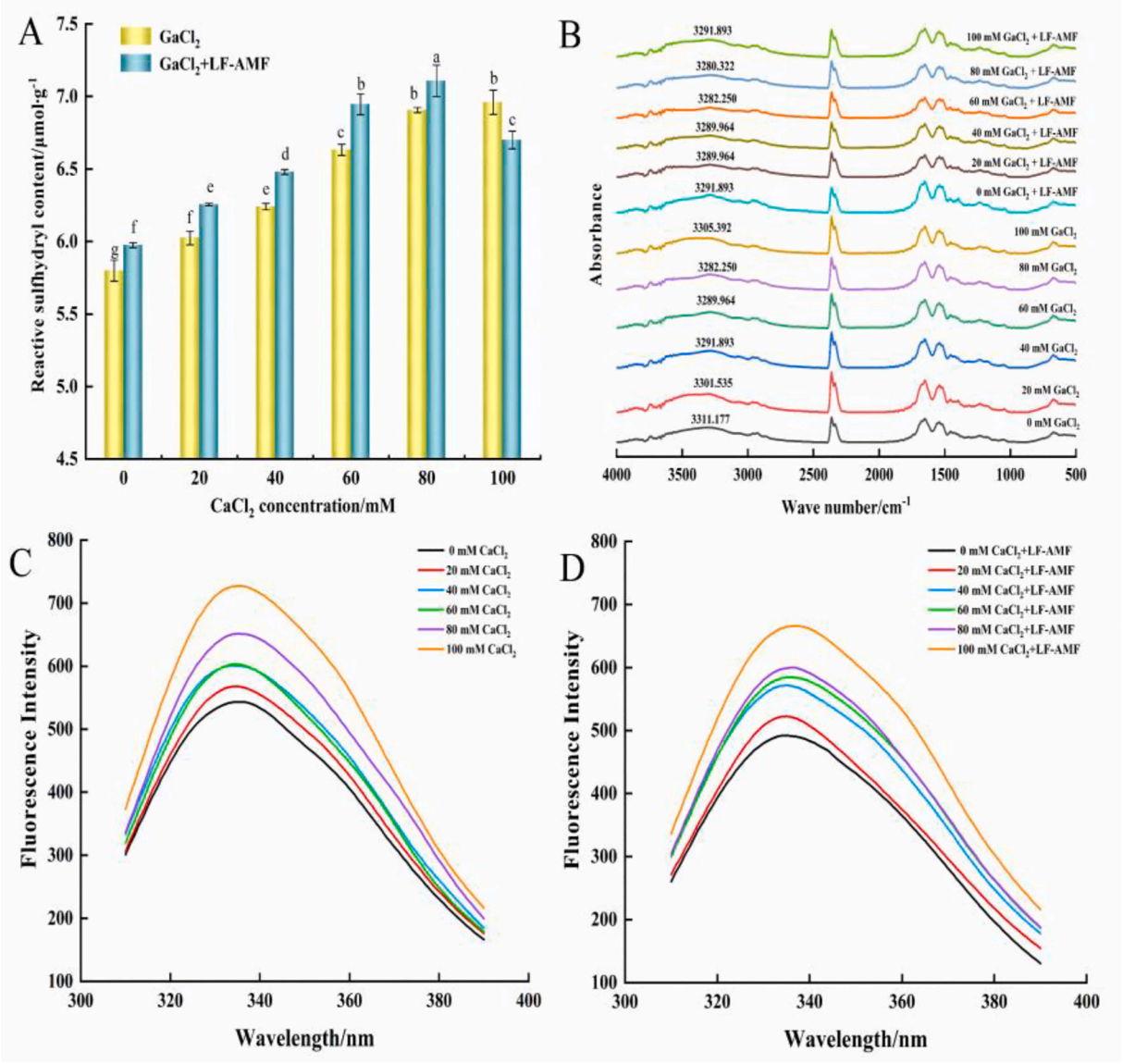

Fig. 2. Effects of LF-AMF combined with $CaCl_2$ on the active sulfhydryl content (A), FTIR spectroscopy (B) and intrinsic fluorescence spectroscopy (C and D) of MP. Different letters (a-g) indicate significant differences among groups ($P < 0.05$).

2.12. Statistical analysis

Data were analyzed by SPSS v.26.0 (SPSS Inc., Chicago, USA). One-way analysis of variance (ANOVA) and Duncan's multiple range test were used for significance analysis at $P < 0.05$. All data were presented as mean ± standard error (SD), and all variables were measured three times and each repetition contained four levels.

3. Results and discussion

3.1. Turbidity and particle size

The effects of LF-AMF and $CaCl_2$ on MP turbidity and particle size are displayed in Fig. 1A and B. As the $CaCl_2$ incorporation increased, the turbidity and average particle size of non-LF-AMF treatment groups significantly ($P < 0.05$) decreased, and the major peak of particle size distribution shifted toward a smaller size (left shift from 1720 nm at 0 mM $CaCl_2$ to 615 nm at 100 mM $CaCl_2$), which might be due to that $CaCl_2$ might promote the dissolution of MP by increasing the ionic strength, and the protein was more evenly dispersed, contributing to the decrease in turbidity and particle size (Wang et al., 2018; Zou, Kang, Li, & Ma, 2022). Another reason might be that the aggregation of Ca^{2+} on the MP surface can generate hydration repulsion between proteins and prevent MP aggregation, resulting in the smaller particle (Wang, Xia, Zhou, Wang, et al., 2020a).

As shown in Fig. 1A and B, the turbidity and average particle size of MP on the similar $CaCl_2$ incorporation with LF-AMF treatments were significantly lower ($P < 0.05$) than the control, and the major peak of particle size distribution further moved to the small size. This might be due to that the LF-AMF can induce MP rearrangement and promote the degradation of partially unstable aggregates, thereby reducing the turbidity (Yang, Wang, et al., 2020). Deng et al. (2021) found that ultrasonic treatment facilitated the rearrangement of protein subunits by hydrophobic interaction, resulting in increased stability of the MP solution. Moreover, Xia et al. (2020) reported similar results, where magnetic field treatment decreased the average particle size of myoglobin, attributing to the redistribution of particle size and the left displacement of the main peak. Previous studies have revealed that the small particle diameter and large surface area of proteins were beneficial to enhancing the interaction of protein-water, yielding desirable

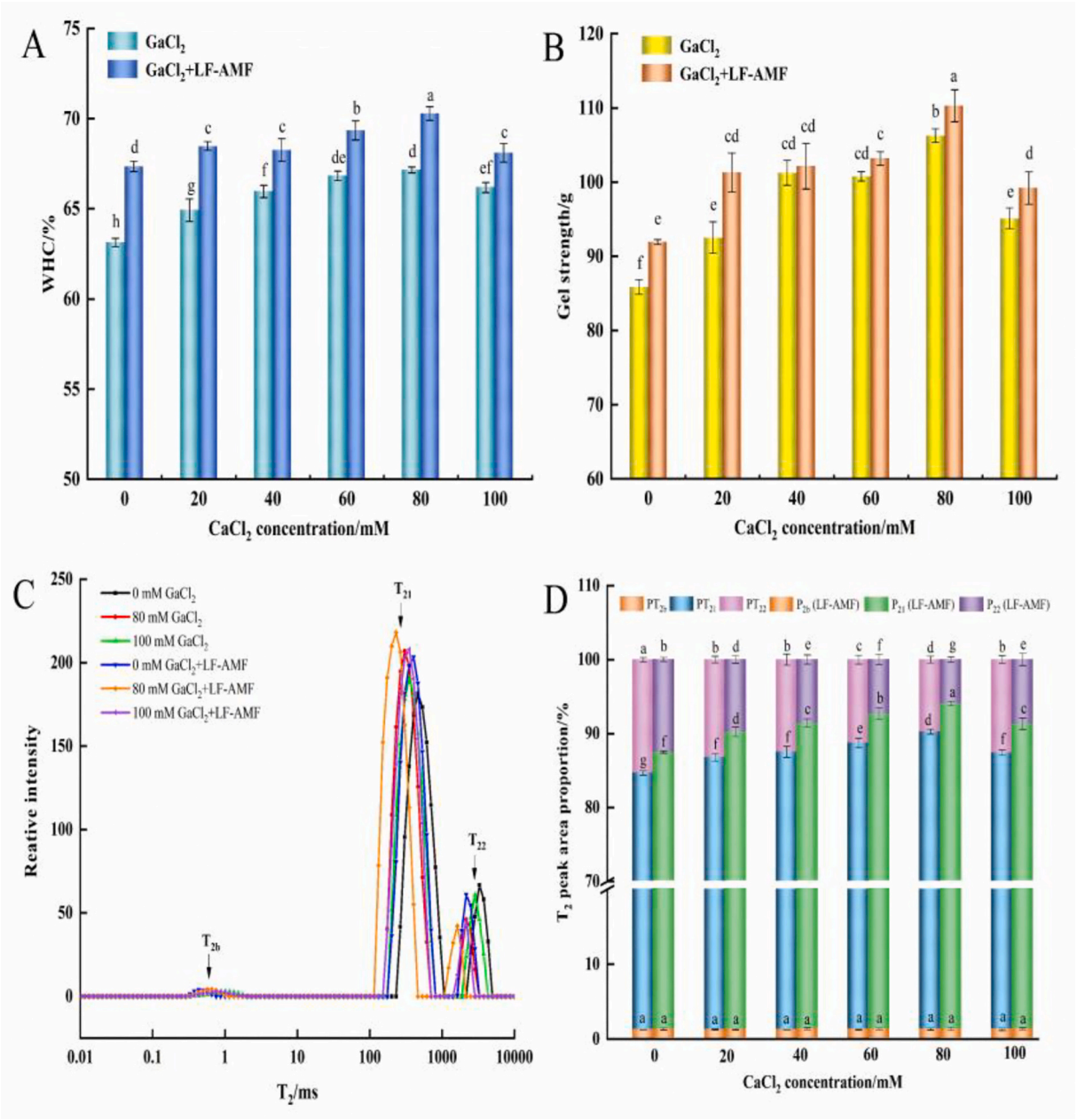

Fig. 3. Effects of LF-AMF combined with $CaCl_2$ on the WHC (A), gel strength (B), T_2 relaxation times (C) and T_2 relaxation peak area proportion (D) of MP. Different letters (a-h) indicate significant differences among groups ($P < 0.05$).

functional properties of proteins (Wang, Xia, Zhou, Wang, et al., 2020a). Thus, compared with individual treatment, LF-AMF combined with $CaCl_2$ effectively reduced the aggregation and particle size of MP.

3.2. Solubility

The solubility of non-LF-AMF treatment groups significantly increased from 10.38% to 40.47% with the increased $CaCl_2$ (Fig. 1C), which was consistent with the findings of turbidity (Fig. 1A) and particle size (Fig. 1B). The results indicating that $CaCl_2$ promote the dissolution of MP attributing to the increased ionic strength of the solution (Zou et al., 2022). Wang et al. (2018) reported similar results that the Ca^{2+} with positive charges can be adsorbed on the MP surface with negative charges, hindered protein aggregation by enhancing hydration repulsion by the formation of hydration layers, increasing in solubility of chicken breast MPs.

The solubility of MP on the similar $CaCl_2$ incorporation with LF-AMF treatment was remarkably higher ($P < 0.05$) than the control, indicating that LF-AMF could further promote the solubilization of $CaCl_2$-MP. This phenomenon could be explained that LF-AMF treatment increased electrostatic repulsion between MP and decreased aggregation of MP, resulting in an increase in solubility (Fabiana et al., 2019; Xia et al., 2020). Besides, the LF-AMF might affect the balance of repulsion and attraction in the solution, increasing solubility (Deng et al., 2021). It has been reported that the treatment with electromagnetic fields could also affect the hydration layer of proteins (Nandi, Futera, & English, 2016). The results were consistent with the study of Amiri, Sharifian, and Soltanizadeh (2018), where ultrasonic treatment could increase the solubility of MP by enhancing protein-water interaction.

3.3. Surface hydrophobicity

The surface hydrophobicity of non-LF-AMF treatment groups remarkably ($P < 0.05$) increased with the increased incorporation of $CaCl_2$ (Fig. 1D) and the maximum value (73.692 μg) was obtained at the 100 mM incorporation of $CaCl_2$. This phenomenon could be explained that calcium ions can induce MP unfolding, facilitated the transfer of non-polar groups to water, resulting in hydrophobic group exposure (An et al., 2018). Wang et al. (2018) found similar results, where $CaCl_2$ induced conformational changes in chicken breast MPs and exposed the internal hydrophobic residues, resulting in increased surface hydrophobicity. Wang, Li, Wang, Xu, and Zeng (2021) also reported that the presence of calcium ions can enhance hydrophobic interactions by unfolding proteins and exposing hydrophobic amino acids.

In addition, under the same $CaCl_2$ incorporation, LF-AMF treatments showed the higher surface hydrophobicity than that of control (Fig. 1D). Compared with the non-magnetic field treatments, the surface hydrophobicity of LF-AMF treatments increased by 21.65 μg and 18.49 μg on 60 mM and 80 mM incorporation of $CaCl_2$, respectively. The increasing surface hydrophobicity indicated that LF-AMF promoted the further change of MP conformation, which was in accordance with the findings of Yang, Wang, et al. (2020), where the magnetic field induced the unfolding of MP, leading to the increase of surface hydrophobicity. The study by Guo, Zhou, et al. (2019) showed that tryptophan and tyrosine could be exposed from the interior of the MP by magnetic field modification. Thus, LF-AMF combined with $CaCl_2$ can contribute to the incremental surface hydrophobicity of MP.

3.4. Active sulfhydryl content

The active sulfhydryl content of MP increased with the increased $CaCl_2$ incorporation without LF-AMF treatment (Fig. 2A). All the $CaCl_2$ treatment groups exhibited higher active sulfhydryl content than the $CaCl_2$-free groups, which may be ascribed to MP unfolding induced by Ca^{2+}, facilitating the sulfhydryl groups exposure (Wang et al., 2018). Another reason might be that the decreased particle size and increased surface area of MP induced more exposure of reactive sulfhydryl groups (Li et al., 2021). The results were similar to the finding by Xiao et al. (2020), where adding $CaCl_2$ could increase the active sulfhydryl content of cellulose nanocrystals-whey protein isolate.

The active sulfhydryl content of LF-AMF treatments was remarkably ($P < 0.05$) higher than non- LF-AMF treatments with the increased $CaCl_2$ from 0 to 80 mM which was consistent with the findings of surface hydrophobicity (Fig. 1D). Yang et al. (2021) found that magnetic field treatment can increase the active sulfhydryl content of MP, which implied that under suitable $CaCl_2$ incorporation (0–80 mM) conditions, the magnetic field could further expose the internal active groups by inducing MP denaturation and expansion of the side-chain groups by $CaCl_2$ incorporation (0–80 mM) (Yang, Wang, et al., 2020). In addition, LF-AMF treatment might alter the MP conformation by modifying the physical properties of water molecules (Zhao, Liu, et al., 2022). However, it is worth noting that when the incorporation of $CaCl_2$ was 100 mM, the active sulfhydryl content of the LF-AMF treatment groups was significantly lower than the non- LF-AMF groups ($P < 0.05$), which could be explained that the magnetic field can not only induce the protein structure unfolding, but also contribute to the MP cross-linking and rearrangement, resulting in the burying of the exposed active residues inside the protein (Yang et al., 2021).

3.5. FTIR spectroscopy

FTIR spectroscopy is a common method for evaluating the changes in protein conformation. The FTIR spectroscopy at 3000–3500 cm^{-1} represents the N—H or O—H stretching of the amide A band, and the lower peak wavenumber indicates stronger protein-water interactions (Zhao, Liu, et al., 2022). As shown in Fig. 2B, the peak wavenumber of the amide A band shifts to a lower wavenumber with the increased $CaCl_2$ from 0 to 80 mM without LF-AMF treatment. Furthermore, the maximum shifting was obtained at 80 mM CaC_2, indicating the strongest protein-water interactions, which was consistent with the results of WHC (Fig. 3A). Ma et al. (2012) reported similar results, where $CaCl_2$ induced an increase of salt-soluble meat protein intramolecular hydrogen bond, leading to the decreased peak wavenumber of amide A band. However, the peak wavenumber of the amide A band of LF-AMF treatment groups with similar $CaCl_2$ incorporation was lower than Non-LF-AMF groups, which indicates that LF-AMF treatment can further enhance the intramolecular hydrogen bonding of MP, which exhibited the same trends as our previous results (Zhao, Liu, et al., 2022).

The Amide *I* band (1600–1700 cm^{-1}) is a sensitive region in the protein secondary structure mainly used to determine the C═O and C═H stretching vibrations in protein structures (Deng et al., 2021). As depicted in Table 1, the content of α-helix and random coil significantly decreased, and the content of β-sheet significantly increased by $CaCl_2$ incorporation from 0 to 100 mM without LF-AMF treatment ($P < 0.05$). The possible reason may be explained that $CaCl_2$, as a divalent salt, can be used as a modifier for protein secondary structure conversion (Zhao, Mu, Zhang, & Richel, 2018). Xiao et al. (2020) and Wang, Xia, Zhou, Wang, et al. (2020a) found that $CaCl_2$ can effectively promote the decrease of α-helix and the increase of β-sheet, contributing to the improvement of the thermal gel formation ability of proteins. Pan et al. (2017) also found that the increased β-sheet and the decreased α-helix were responsible for the improved WHC of MP, which was consistent with the present results. Interestingly, the content of α-helix and β-turn exhibited a significant decrease by LF-AMF treatment with similar $CaCl_2$ incorporation ($P < 0.05$), while the content of β-sheet and random coil exhibited a significant increase ($P < 0.05$), which was consistent with our previous results (Zhao, Liu, et al., 2022). This phenomenon can be attributed to the further modification of the protein secondary structure by LF-AMF treatment, which induces MP unfolding, leading to exposing

Table 1
Effects of LF-AMF combined with $CaCl_2$ on the secondary structure content of MP.

samples	$GaCl_2$ concentration/ mM	Proportion/%			
		α-Helix	β-Sheet	β-turn	random coil
$GaCl_2$	0	23.137 ± 0.203^{a}	36.341 ± 0.405^{g}	21.342 ± 0.163^{b}	19.181 ± 0.411^{cd}
	20	21.557 ± 0.503^{b}	37.206 ± 0.086^{f}	21.912 ± 0.071^{a}	19.324 ± 0.415^{bcd}
	40	21.092 ± 0.060^{c}	38.280 ± 0.292^{e}	21.566 ± 0.115^{ab}	19.062 ± 0.229^{cde}
	60	19.833 ± 0.194^{f}	40.074 ± 0.188^{d}	21.481 ± 0.316^{ab}	18.611 ± 0.070^{d}
	80	19.543 ± 0.080^{fg}	40.749 ± 0.359^{c}	21.588 ± 0.175^{ab}	18.121 ± 0.283^{f}
	100	20.380 ± 0.068^{e}	38.306 ± 0.069^{e}	21.884 ± 0.122^{a}	19.431 ± 0.014^{bc}
$GaCl_2$+ LF-AMF	0 + LF-AMF	21.095 ± 0.131^{c}	40.030 ± 0.081^{d}	18.678 ± 0.055^{c}	20.197 ± 0.068^{a}
	20+ LF-AMF	20.844 ± 0.156^{cd}	41.043 ± 0.671^{c}	18.040 ± 0.278^{d}	20.073 ± 0.265^{a}
	40+ LF-AMF	20.473 ± 0.385^{de}	41.736 ± 0.748^{b}	18.020 ± 0.495^{d}	19.770 ± 0.472^{ab}
	60+ LF-AMF	19.367 ± 0.176^{g}	42.963 ± 0.443^{a}	18.390 ± 0.428^{cd}	19.280 ± 0.058^{bcd}
	80+ LF-AMF	18.877 ± 0.182^{h}	43.575 ± 0.173^{a}	18.707 ± 0.342^{c}	18.841 ± 0.087^{de}
	100+ LF-AMF	20.686 ± 0.312^{cde}	40.914 ± 0.224^{c}	18.848 ± 0.163^{c}	19.552 ± 0.247^{bc}

Different letters (a-h) of the same column indicate significant differences between groups ($P < 0.05$).

more active groups and promoting protein structure rearrangement (Zhao, Liu, et al., 2022). Wang et al. (2020) found that magnetic field treatment caused the destruction of hydrogen bonds between carbonyl and acylamino in α-helix, leading to a decrease in α-helix content.

3.6. Intrinsic fluorescence spectroscopy

As depicted in Fig. 2C, the intrinsic fluorescence intensity of MP gradually increased at 335 nm with the increased $CaCl_2$ without LF-AMF treatment, and obtained a maximum value at 100 mM, which indicated that $CaCl_2$ altered the tertiary structure of MP. These results can be ascribed that the $CaCl_2$ might enhance the ionic strength of the solution, thus affecting the polar microenvironment of tryptophan, resulting in the change of the tertiary structure (Ren et al., 2022). The results were similar to the finding by Xiao et al. (2020) reported the similar finding, where Ca^{2+} (0–0.15 M) increased the fluorescence intensity of cellulose nanocrystals-whey protein isolate. Zou et al. (2019) reported that protein structure unfolding and hydrophobic bond destruction may also lead to an increase in intrinsic fluorescence intensity.

Interestingly, as shown in Fig. 2D, the intrinsic fluorescence intensity of MP exhibited a decreased trend by LF-AMF treatment with the same $CaCl_2$ incorporation, which was opposite to the trend of using $CaCl_2$ alone. This phenomenon was likely attributed to the magnetic field modification of the tertiary structure of MP, altering the microenvironment of protein residues (Yang, Wang, et al., 2020). In addition, the fluorescence quenching induced by the interaction between the magnetic field and MP also contributed to the decrease of the fluorescence intensity. Similarly, high-pressure treatment induced a weak fluorescence intensity by shortening the distance between tryptophan residues and quenching residues (cysteine, lysine, and histidine) (Wang, Xia, Zhou, Wang, et al., 2020b). Zou et al. (2019) also found that the combination of ultrasound and sodium bicarbonate altered the polar microenvironment of proteins and induced energy transfer, leading to decreased fluorescence intensity.

3.7. Gel properties

3.7.1. WHC

As displayed in Fig. 3A, the WHC of the non-LF-AMF treatment groups exhibited an initially increase and then decreased trend with the increased $CaCl_2$, and the maximum value (67.15%) was obtained at 80 mM. These results indicated that the incorporation of $CaCl_2$ could improve the water retention of MP, which is probably because that $CaCl_2$ can alter the MP conformation, promote protein cross-linking during the formation of thermal gelation, and induce the formation of a desirable gel network structure, contributing to the entrapment of more water molecules (Wang, Xia, Zhou, Wang, et al., 2020a; Xiao et al., 2020). Additionally, the decrease of pore size in protein gels facilitates to enhancement of the capillary force and the resistance capability on external pressure, resulting in the improvement of WHC (Zhong et al., 2020). Similar findings were reported by Guo, Li, et al. (2019), where adding $CaCl_2$ increased the WHC of golden threadfin bream myosin. However, the WHC of MP remarkably decreased when the added amount of $CaCl_2$ reached 100 mM ($P < 0.05$), which might be due to the fact that excessive Ca^{2+} hinders the penetration of NaCl into protein, resulting in a decrease in water retention of protein (Zheng et al., 2019).

The WHC of LF-AMF treatment groups on the same $CaCl_2$ incorporation was distinctly higher than control groups ($P < 0.05$), which may be ascribed to the unfolding and ordered aggregation of MP side chains generated by LF-AMF treatment, promoting the interaction between MP and water for forming a compact gel network structure (Zhong et al., 2020). Yang et al. (2020) reported that LF-AMF treatment induced the MP rearrangement and the exposure of the water-binding sites involved in hydrogen bonding, contributing to an increase in WHC. The homogeneous and orderly gel network structure of MP induced by LF-AMF treatment was also responsible for the increase in WHC (Yang, Zhou, et al., 2020). Moreover, the enhanced surface hydrophobicity and active sulfhydryl groups (Figs. 1D and 2A) after LF-AMF treatment may also be involved in the interaction of protein-water and protein-protein, promoting the high WHC of MP gels (Yang, Wang, et al., 2020).

3.7.2. Gel strength

The gel strength of the non-LF-AMF treatment groups exhibited an initially increase and then decreased trend with the increased $CaCl_2$, and obtained a maximum value (106.21 g) at 80 mM (Fig. 3B). These results are likely due to the formation of the salt bridge induced by $CaCl_2$, strengthened the cross-linking during MP thermal gelation, facilitating to form a dense gel structure (Xiao et al., 2020). Moreover, more cross-linking sites were exposed because of protein unfolding, contributing to the protein-protein interaction (Guo, Li, et al., 2019). Nevertheless, the gel strength of MP distinctly decreased when the incorporation of $CaCl_2$ reached 100 mM ($P < 0.05$), which is probably because that excessive Ca^{2+} induced a large number of positive charges in the MP gels system, resulting in the repulsion or dissociation between MP molecules and weakening the gel structure (Zhao et al., 2018).

The gel strength of the LF-AMF treatment groups with the same $CaCl_2$ incorporation was distinctly ($P < 0.05$) higher than the non-LF-AMF treatment groups, indicating that LF-AMF treatment could induce MP to form a more compact gel structure resulting in the improvement of gel strength (Guo, Zhou, et al., 2019), which was consistent with the results of WHC (Fig. 3A). Similar findings were reported by Wu et al. (2021), where the magnetic field could improve the gel strength of MP at different temperature. Zhao, Liu, et al. (2022) found that the enhancement of gel strength by magnetic field treatment may be attributed to forming a desired gel network structure by changing the charge distribution on the surface of water molecules and protein molecules. Yang, Zhou, et al. (2020) reported an increase in the gel properties by magnetic field treatment, which was probably caused by exposing hydrophobic residues to participate in the hydrogen bonding of water. Thus, LF-AMF combined with $CaCl_2$ treatment could effectively improve the gel strength of MP.

3.7.3. LF-NMR

Low-field NMR is commonly used to evaluate the water distribution and migration of meat products. Three NMR characteristic peaks were observed in low-salt MP gel (T_{2b}, T_{21}, T_{22}), which represented bound water (0.1–10 ms, T_{2b}) tightly bound to macromolecules, immobilized water in MP gel network (100–1000 ms, T_{21},) and free water outside MP gel network (1000–10,000 ms, T_{22}), respectively (Zhao, Li, et al., 2022). Fig. 3C showed that the peak of T_2 relaxation time exhibited significant shifting. Without LF-AMF treatment, adding $CaCl_2$ could significantly ($P < 0.05$) shorten T_{21} and T_{22}, but did not affect T_{2b}, which was similar to the results reported by Yu, Gong, Yuan, Bao, and Wang (2022), where $CaCl_2$ significantly shortened the relaxation time of immobilized water and free water in surimi gel ($P < 0.05$). It is well known that the decreased relaxation time was closely related to the improvement of the binding capacities of water and macromolecules (Yang, Zhou, et al., 2020). Therefore, these results indicated that adding $CaCl_2$ enhanced the binding capacities between water and protein, contributing to an increase in WHC. However, the position of T_{21} and T_{22} of MP gel shifted to higher relaxation times at 100 mM $CaCl_2$, which may be attributed to the promotion of the flow of water by the large gel pores (Fig. 5C and F). In addition, the T_{21} and T_{22} of the LF-AMF treatment groups on the same $CaCl_2$ incorporation were shorter than those without LF-AMF treatment, indicating that LF-AMF further reduced the water migration of MP gel and improved the WHC, which maybe because that the magnetic field induces the rearrangement of the charged molecules and promotes the formation of an ordered gel structure, restricting the movement of water molecules (Yang, Zhou, et al., 2020). Moreover, the anther possible explanation is that a magnetic field can decrease water mobility by inducing protein unfolding and promoting protein hydration (Zhao et al., 2018). A similar result was reported by Wang, Zhou, Wang, Li,

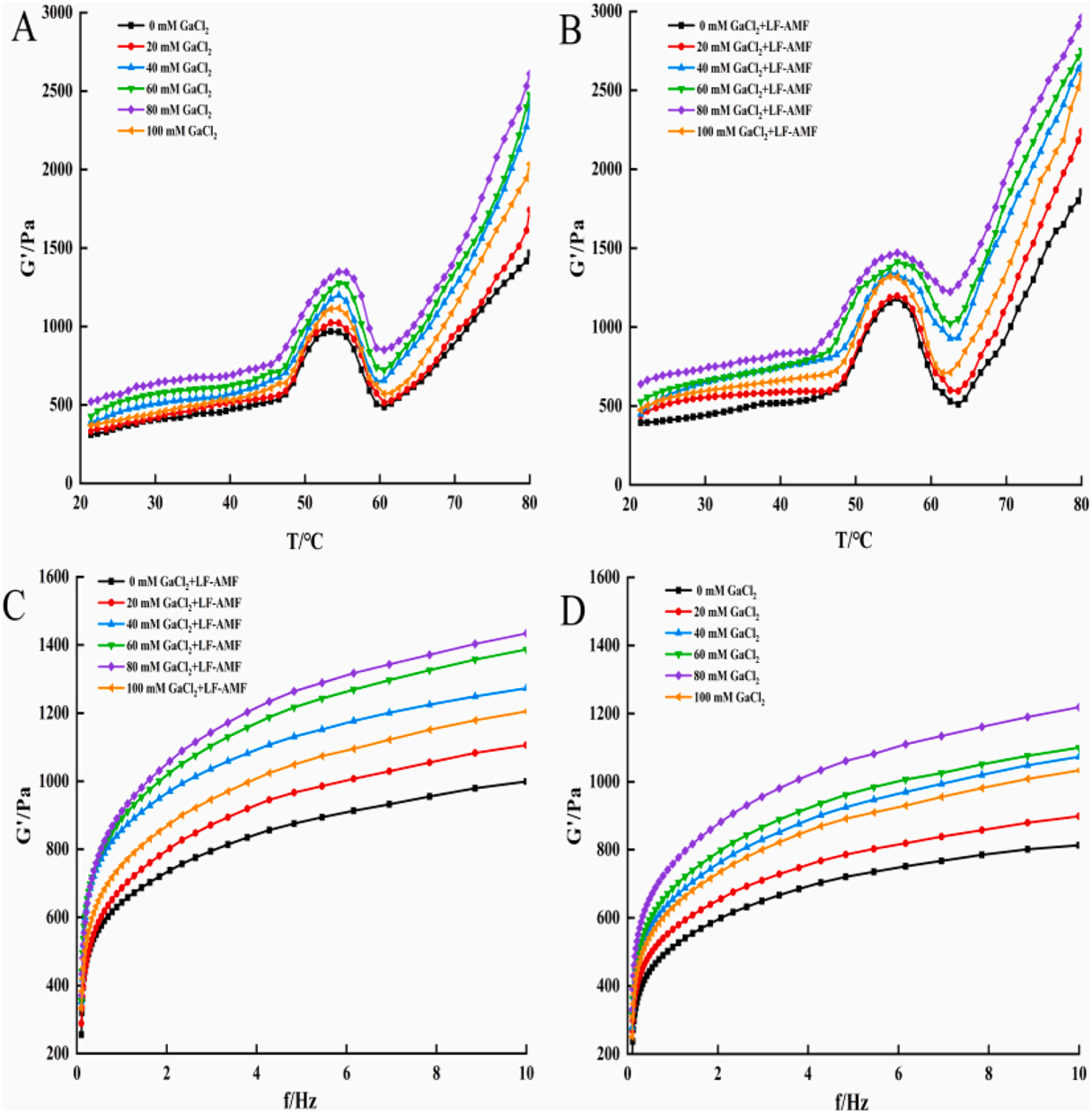

Fig. 4. Effects of LF-AMF combined with $CaCl_2$ on the G' value of MP in temperature scanning (A and B) and frequency scanning (C and D).

et al. (2020), where magnetic field treatment induced a short T_{21}, promoted a close binding between water and MP, resulting in a decrease in water mobility.

The different T_2 intervals corresponding peak area percentages were expressed by P_{2b}, P_{21}, and P_{22}, respectively. No significance in PT_{2b} was observed in Fig. 3D ($P > 0.05$), indicating that $CaCl_2$ and LF-AMF treatment did not influence the content of bound water. Nevertheless, the PT_{21} remarkably increased from 83.43% (0 mM) to 88.96% (80 mM) and the PT_{22} remarkably decreased from 15.32% to 9.74% with the increased $CaCl_2$, respectively ($P < 0.05$). This phenomenon could be because that $CaCl_2$ induces the unfolding of the myosin tail, leading to an improvement of the gel network structure of MP (Guo,Li, et al., 2019). The increased content of immobilized water and the decreased content of free water facilitated to hindering the water migration in MP gel, consistent with the results of WHC (Fig. 3A). Pan et al. (2017) reported similar findings, where adding $CaCl_2$ increased the immobilized water of myosin - κ-carrageenan compounds by entrapping more water molecules in compact gel network structure. However, PT_{21} distinctly decreased and PT_{22} distinctly increased at 100 mM $CaCl_2$ ($P < 0.05$), indicating that excessive $CaCl_2$ induced the transfer of immobilized water from the gel network structure to the outside, leading to a decrease in WHC of the MP gel. In addition, another possible reason is that the excessive crosslinking of MP caused by $CaCl_2$ promotes the formation of rough and loose gel structures, resulting in the weakened water retention capacity of MP gel. LF-AMF treatment with $CaCl_2$ further increased the content of immobilized water and reduced the content of free water (Fig. 3D), which could be attributed to forming a dense MP gel microstructure with uniform and small pores induced by LF-AMF (Fig. 5E), contributing to entrapping more water into the gel network structure and increasing the content of immobilized water (Wang, Zhou, Wang, Ma, et al., 2020). Moreover, the exposure of hydrophobic residues of MP induced by LF-AMF was also responsible for the improvement of immobilized water content (Yang et al., 2021). Wang et al. (2021) reported that pulsed electric fields induced the formation of ordered pores in the microstructure, affecting the water mobility and improving the WHC of chicken breast meat. Consequently,

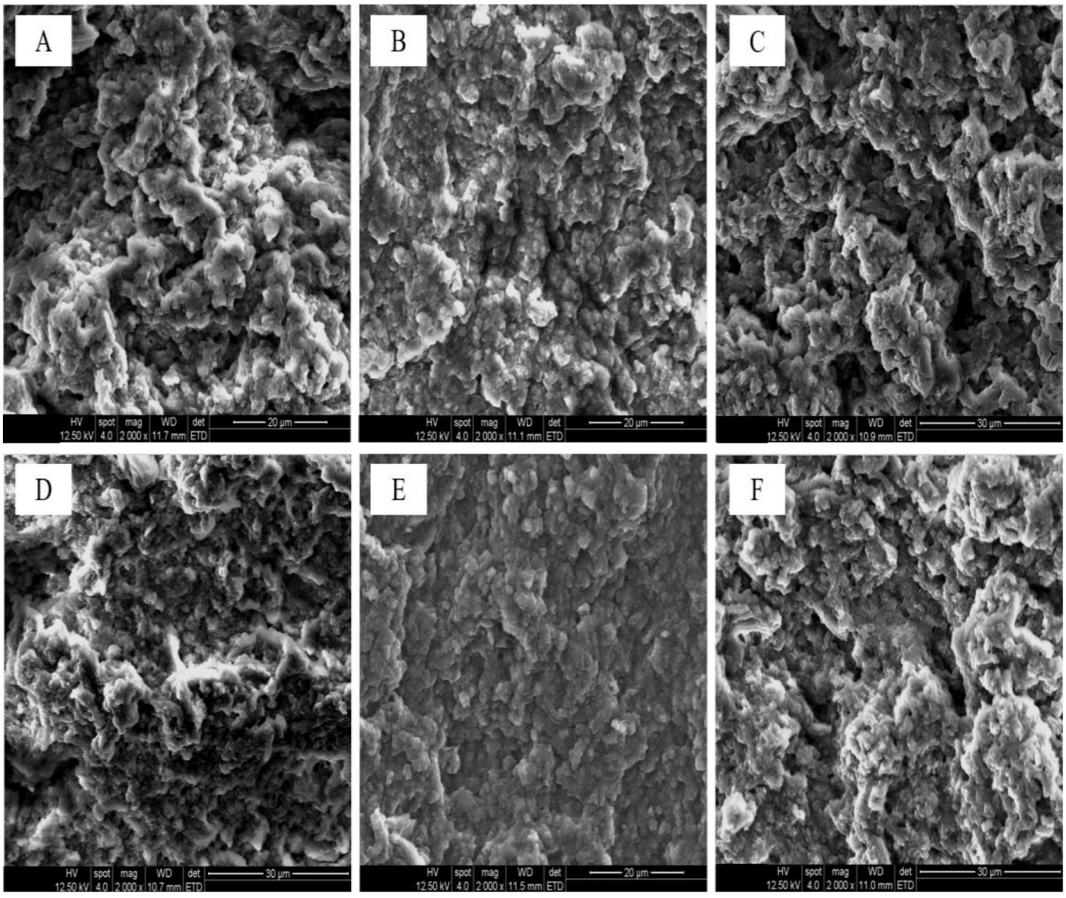

Fig. 5. Effects of LF-AMF combined with $CaCl_2$ on the microstructure of MP. A-C: 0 mM $CaCl_2$, 80 mM $CaCl_2$, 100 mM $CaCl_2$; D-F: 0 mM $CaCl_2$ + LF-AMF, 80 mM $CaCl_2$ + LF-AMF, 100 mM $CaCl_2$ + LF-AMF.

LF-AMF combining $CaCl_2$ can alter the water migration and distribution to improve the WHC of MP gel.

3.7.4. Dynamic rheology

Rheological property is a common method to evaluate protein gelation ability (Gao et al., 2022). The change of storage modulus (G' value) of MP in temperature sweeping is shown in Fi. 4 A and 4B. All samples showed similar trends with the typical rheological curves of MP, containing three main stages: "gel setting", "gel weakening" and "gel strengthening" (Guo, Li, et al., 2019). During the process, MP underwent weak binding of the myosin head, degeneration of the myosin tail, and aggregation of unfolded myosin to form an irreversible gel (Gao et al., 2022). The G' value of MP showed initial increase and then decrease with the increased $CaCl_2$ without LF-AMF treatment during the temperature sweeping from 20 to 80 °C, and obtained the maximum value at 80 mM. The results indicated that $CaCl_2$ promoted to formation of a more stable MP gel network structure, which may due the formation of disulfide bonds and salt bridges by Ca^{2+} and the enhancement of hydrophobic interaction (Hu et al., 2022). These results were consistent with the findings of Zhang, Zhang, Zhong, Qi, and Li (2022), who reported that $CaCl_2$ could induce the soy and whey protein isolate with higher storage modulus, improving the microstructure and water retention. However, excessive calcium salt might cause excessive aggregation of proteins, leading to forming a rough gel structure and reducing the gel elasticity (Xiao et al., 2020). In addition, the G' value of the LF-AMF treatment groups on the same $CaCl_2$ incorporation was higher than the non-LF-AMF treatment groups, indicating that LF-AMF treatment could further modify the elasticity of $CaCl_2$-MP gel, which was consistent with the results of gel strength (Fig. 3B). This phenomenon may be explained that LF-AMF treatment promotes hydrophobic interaction and protein-protein interaction during the thermal gelation process, forming a desirable gel structure (Yang, Zhou, et al., 2020). An et al. (2018) argued that the ultrasound combining calcium treatment improved the G' value of myosin by promoting myosin unfolding.

As shown in Fig. 4C and D, in the absence of LF-AMF treatment, the G' value of MP samples in all groups showed an upward trend with the increased frequency, indicating that the elasticity of MP significantly increased with the increased frequency, which was consistent with the report of Peyrano, de Lamballerie, Avanza, and Speroni (2022) on the changing trend of G' value of HPP-treated cowpea protein. On the other hand, the G' value increased with increasing incorporation of $CaCl_2$ at the same frequency, which may be due to the formation of a salt bridge between the polypeptide induced by Ca^{2+} (Peyrano et al., 2022). A decrease in the critical protein concentration for protein gelation caused by Ca^{2+} may be another reason for the increased G' value (Peyrano, de Lamballerie, Avanza, & Speroni, 2019). However, the excessive incorporation of $CaCl_2$ at 100 mM led to an imbalance of gravity and repulsion in the gel system and a rough gel structure (Fig. 5C and F), resulting in a decrease in the G' value. In addition, LF-AMF treatment increased the G' value and further improved the elastic properties of MP at the same frequency and $CaCl_2$ incorporation. These results were probably because of the decreased average particle size of myofibrillar protein by magnetic field treatment (Fig. 1B). Protein with smaller particle size exhibits a better molecular chain arrangement and facilitates to forming irreversible chemical bonds, promoting to form an elastic-based gel (Amiri et al., 2018). The increase in solubility was conducive to the gel network, which might be one of the reasons for the increase in G' value (Ren et al., 2022). Zhao, Liu, et al. (2022) reported that LF-AMF treatment could promote the formation of elastic gel with a high G' value in pork batter gel, which was in agreement with our results. Hence, the LF-

AMF combined $CaCl_2$ could effectively modify the rheological properties of MP.

3.7.5. Microstructure

The microstructure changes of MP after LF-AMF combined $CaCl_2$ treatment were shown in Fig. 5. The non-$CaCl_2$ samples had a rough and heterogeneous gel-network structure with large aggregates (Fig. 5A and D), which could be attributed to the poor MP solubility without $CaCl_2$ (Fig. 1C), and the emergence of large protein aggregates prior to the formation of stable gel structure during the thermal process, contributing to forming a fragile gel structure (Guo, Li, et al., 2019). The incorporation of $CaCl_2$ induced the formation of a uniform and dense MP gel network structure, which was in accordance with the findings of Hu et al. (2022), where a dense and homogeneous gel network structure of sliver carp myosin was obtained by adding $CaCl_2$. Besides, Ca^{2+} could facilitate the formation of a protein gel network by reducing electrostatic repulsion and forming a salt bridge (Xiao et al., 2020). When the incorporation of $CaCl_2$ reached 100 mM, greater protein aggregation was formed in the MP gel network structure (Fig. 5C and F), which could be because of the imbalance of various interactions (electrostatic interaction, hydrophobic interaction, disulfide bond, and hydrogen bond) between proteins induced by excessive Ca^{2+} (Ma et al., 2012).

Furthermore, the microstructure of LF-AMF treatment groups was more compact and uniform at the same $CaCl_2$ incorporation, which may be attributed to the charged MP rearrangement caused by the magnetic field (Yang, Zhou, et al., 2020). Wang, Zhou, Wang, Ma, et al. (2020) noted that magnetic field treatment accelerated the unfolding and orderly aggregation of grass carp MP, promoted to form a uniform and dense gel structure, resulting in the improving WHC. Therefore, the LF-AMF combined $CaCl_2$ could effectively facilitate the formation of a desired gel network structure of MP and improve the gel quality.

4. Conclusion

In the present study, LF-AMF (5mT) combined with $CaCl_2$ treatment could effectively ameliorate the gel characteristics of low-salt MP by modifying protein conformation. Adding $CaCl_2$ at 80 mM $CaCl_2$ showed increased MP solubility, surface hydrophobicity, and exposure of active sulfhydryl, reduced particle size, α-helix unfolded to form the β-sheet, thereby forming a desired gel structure to entrap more water, and ultimately improve WHC. However, $CaCl_2$ (100 mM) caused excessive cross-linking of MP to form a rough gel microstructure, contributing to a decreased G' value, WHC, and gel strength. Interestingly, LF-AMF treatment further heightens the beneficial effects for improving the gel characteristics of low-salt MP. Therefore, the combined treatment of LF-AMF and $CaCl_2$ could be a promising and efficient technique for ameliorating the gel qualities of low-salt meat products.

CRediT authorship contribution statement

Shengming Zhao: Writing – original draft, Funding acquisition. **Yu Liu:** Methodology, Software. **Liu Yang:** Methodology. **Yanyan Zhao:** Resources, Supervision. **Mingming Zhu:** Investigation. **Hui Wang:** Conceptualization. **Zhuangli Kang:** Resources. **Hanjun Ma:** Funding acquisition, Project administration.

Declaration of competing interest

The authors declare that they do not have any conflict of interest.

Data availability

Data will be made available on request.

Acknowledgments

The authors would like to thank the financial support received from the Major Science and Technology Special Project of Henan province (grant no. 221100110500) and Key Scientific and Technological Projects in the Henan Province of China (grant no. 232102111056).

References

Amiri, A., Sharifian, P., & Soltanizadeh, N. (2018). Application of ultrasound treatment for improving the physicochemical, functional and rheological properties of myofibrillar proteins. *International Journal of Biological Macromolecules, 111*, 139–147.

An, Y., Liu, Q., Xie, Y., Xiong, S., Yin, T., & Liu, R. (2018). Aggregation and conformational changes of silver carp myosin as affected by ultrasound-calcium combination system. *Journal of the Science of Food and Agriculture, 98*(14), 5335–5343.

Deng, X., Ma, Y., Lei, Y., Zhu, X., Zhang, L., Hu, L., Lu, S., Guo, X., & Zhang, J. (2021). Ultrasonic structural modification of myofibrillar proteins from Coregonus peled improves emulsification properties. *Ultrasonics Sonochemistry, 76*(6), Article 105659.

Fabiana, L. S., Guilherme, Z., Katia, R., Luana, C. L., Lídia, T., Lenilton, S. S., … O., & Marco, D. L.. (2019). Changes in the physico-chemical characteristics of a protein solution in the presence of magnetic field and the consequences on the ultrafiltration performance. *Journal of Food Engineering, 242*, 84–93.

Gao, Y., Luo, C., Zhang, J., Wei, H., Zan, L., & Zhu, J. (2022). Konjac glucomannan improves the gel properties of low salt myofibrillar protein through modifying protein conformation. *Food Chemistry, 393*, Article 133400.

Guo, J., Zhou, Y., Yang, K., Yin, X., Ma, J., Li, Z., Sun, W., & Han, M. (2019). Effect of low-frequency magnetic field on the gel properties of pork myofibrillar proteins. *Food Chemistry, 274*, 775–781.

Guo, Z., Li, Z., Wang, J., & Zheng, B. (2019). Gelation properties and thermal gelling mechanism of golden threadfin bream myosin containing $CaCl_2$ induced by high pressure processing. *Food Hydrocolloids, 95*, 43–52.

Hu, Y., Zhang, M., Zhao, Y., Gao, X., You, J., Yin, T., Xiong, S., & Liu, R. (2022). Effects of different calcium salts on the physicochemical properties of sliver carp myosin. *Food Bioscience, 47*, Article 101518.

Li, Y., Zhang, X., Lu, F., & Kang, Z. (2021). Effect of sodium bicarbonate and sodium chloride on aggregation and conformation of pork myofibrillar protein. *Food Chemistry, 350*, Article 129233.

Ma, F., Chen, C., Sun, G., Wang, W., Fang, H., & Han, Z. (2012). Effects of high pressure and $CaCl_2$ on properties of salt-soluble meat protein gels containing locust bean gum. *Innovative Food Science and Emerging Technologies, 14*, 31–37.

Nandi, P. K., Futera, Z., & English, N. J. (2016). Perturbation of hydration layer in solvated proteins by external electric and electromagnetic fields: Insights from non-equilibrium molecular dynamics. *Journal of Chemical Physics, 145*(20), 93–172.

Pan, T., Guo, H., Li, Y., Song, J., & Ren, F. (2017). The effects of calcium chloride on the gel properties of porcine myosin–κ-carrageenan mixtures. *Food Hydrocolloids, 63*, 467–477.

Peyrano, F., de Lamballerie, M., Avanza, M. V., & Speroni, F. (2019). Rheological characterization of the thermal gelation of cowpea protein isolates: Effect of pretreatments with high hydrostatic pressure or calcium addition. *LWT - Food Science and Technology, 115*, Article 108472.

Peyrano, F., de Lamballerie, M., Avanza, M. V., & Speroni, F. (2022). High hydrostatic pressure- or heat-induced gelation of cowpea proteins at low protein content: Effect of calcium concentration. *Food Hydrocolloids, 124*, Article 107220.

Ren, Z., Cui, Y., Wang, Y., Shi, L., Yang, S., Hao, G., Qiu, X., Wu, Y., Zhao, Y., & Weng, W. (2022). Effect of ionic strength on the structural properties and emulsion characteristics of myofibrillar proteins from hairtail (*Trichiurus haumela*). *Food Research International, 157*, Article 111248.

Wang, J., Li, J., Wang, R., Xu, F., & Zeng, X. (2021). Improving water retention of chicken breast meats by $CaCl_2$ combined with pulsed electric fields. *International Journal of Food Science & Technology, 57*(2), 791–800.

Wang, K., Li, Y., Zhang, Y., Luo, X., & Sun, J. (2022). Improving myofibrillar proteins solubility and thermostability in low-ionic strength solution: A review. *Meat Science, 189*, Article 108822.

Wang, L., Xia, M., Zhou, Y., Wang, X., Ma, J., Xiong, G., Wang, L., Wang, S., & Sun, W. (2020b). Gel properties of grass carp myofibrillar protein modified by low-frequency magnetic field during two-stage water bath heating. *Food Hydrocolloids, 107*, Article 105920.

Wang, X., Xia, M., Zhou, Y., Wang, L., Feng, X., Yang, K., Ma, J., Li, Z., Wang, L., & Sun, W. (2020a). Gel properties of myofibrillar proteins heated at different heating rates under a low-frequency magnetic field. *Food Chemistry, 321*, 126–728.

Wang, Y., Zhou, Y., Li, P., Wang, X., Cai, K., & Chen, C. (2018). Combined effect of $CaCl_2$ and high pressure processing on the solubility of chicken breast myofibrillar proteins under sodium-reduced conditions. *Food Chemistry, 269*, 236–243.

Wang, Y., Zhou, Y., Wang, X., Li, P., Xu, B., & Chen, C. (2020). Water holding capacity of sodium-reduced chicken breast myofibrillar protein gel as affected by combined $CaCl_2$ and high-pressure processing. *International Journal of Food Science & Technology, 55*(2), 601–609.

Wang, Y., Zhou, Y., Wang, X., Ma, F., Xu, B., Li, P., & Chen, C. (2020). Origin of high-pressure induced changes in the properties of reduced-sodium chicken myofibrillar protein gels containing $CaCl_2$: Physicochemical and molecular modification perspectives. *Food Chemistry, 319*, Article 126535.

Wu, D., Guo, J., Wang, X., Yang, K., Wang, L., Ma, J., Zhou, Y., & Sun, W. (2021). The direct current magnetic field improved the water retention of low-salt myofibrillar protein gel under low temperature condition. *LWT - Food Science and Technology, 151*, Article 112034.

Xia, M., Chen, Y., Ma, J., Yin, X., Wang, L., Wu, W., Xiong, G., Sun, W., & Zhou, Y. (2020). Effects of low frequency magnetic field on myoglobin oxidation stability. *Food Chemistry, 309*, Article 125651.

Xiao, Y., Kang, S., Liu, Y., Guo, X., Li, M., & Xu, H. (2020). Effect and mechanism of calcium ions on the gelation properties of cellulose nanocrystals-whey protein isolate composite gels. *Food Hydrocolloids, 111*, Article 106401.

Yang, K., Wang, H., Huang, J., Wu, D., Zhao, M., Ma, J., & Sun, W. (2020). Effects of direct current magnetic field treatment time on the properties of pork myofibrillar protein. *International Journal of Food Science & Technology, 56*(2), 733–741.

Yang, K., Wang, L., Guo, J., Wu, D., Wang, X., Wu, M., Feng, X., Ma, J., Zhang, Y., & Sun, W. (2021). Structural changes induced by direct current magnetic field improve water holding capacity of pork myofibrillar protein gels. *Food Chemistry, 345*, Article 128849.

Yang, K., Zhou, Y., Guo, J., Feng, X., Wang, X., Wang, L., Ma, J., & Sun, W. (2020). Low frequency magnetic field plus high pH promote the quality of pork myofibrillar protein gel: A novel study combined with low field NMR and Raman spectroscopy. *Food Chemistry, 326*, Article 126896.

Yu, N., Gong, H., Yuan, H., Bao, Y., & Wang, W. (2022). Effects of calcium chloride as a salt substitute on physicochemical and 3D printing properties of silver carp surimi gels. *CyTA Journal of Food, 20*(1), 1–12.

Zhang, X., Zhang, S., Zhong, M., Qi, B., & Li, Y. (2022). Soy and whey protein isolate mixture/calcium chloride thermally induced emulsion gels: Rheological properties and digestive characteristics. *Food Chemistry, 380*, Article 132212.

Zhao, S., Li, Z., Liu, Y., Zhao, Y., Yuan, X., Kang, Z., Zhu, M., & Ma, H. (2022). High-pressure processing influences the conformation, water distribution, and gel properties of pork myofibrillar proteins containing *Artemisia sphaerocephala Krasch* gum. *Food Chemistry: X, 14*, Article 100320.

Zhao, S., Liu, Y., Yuan, X., Zhao, Y., Kang, Z., Zhu, M., & Ma, H. (2022). Effect of low-frequency alternating magnetic field on the rheological properties, water distribution and microstructure of low-salt pork batters. *LWT - Food Science and Technology, 159*, Article 113164.

Zhao, Z., Mu, T., Zhang, M., & Richel, A. (2018). Effect of salts combined with high hydrostatic pressure on structure and gelation properties of sweet potato protein. *LWT - Food Science and Technology, 93*, 36–44.

Zheng, J., Han, Y., Ge, G., Zhao, M., & Sun, W. (2019). Partial substitution of NaCl with chloride salt mixtures: Impact on oxidative characteristics of meat myofibrillar protein and their rheological properties. *Food Hydrocolloids, 96*, 36–42.

Zhong, M., Xie, F., Zhang, S., Sun, Y., Qi, B., & Li, Y. (2020). Preparation and digestive characteristics of a novel soybean lipophilic protein-hydroxypropyl methylcellulose-calcium chloride thermosensitive emulsion gel. *Food Hydrocolloids, 106*, Article 105891.

Zou, X., Kang, Z., Li, Y., & Ma, H. (2022). Effect of sodium bicarbonate on solubility, conformation and emulsion properties of pale, soft and exudative meat myofibrillar proteins. *LWT - Food Science and Technology, 157*, Article 113097.

Zou, Y., Shi, H., Xu, P., Jiang, D., Zhang, X., Xu, W., & Wang, D. (2019). Combined effect of ultrasound and sodium bicarbonate marination on chicken breast tenderness and its molecular mechanism. *Ultrasonics Sonochemistry, 59*, Article 104735.

Zou, Y., Yang, H., Li, P., Zhang, M., Zhang, X., Xu, W., & Wang, D. (2019). Effect of different time of ultrasound treatment on physicochemical, thermal, and antioxidant properties of chicken plasma protein. *Poultry Science, 98*(4), 1925–1933.